Original Research Article

Synthesis, *In Vitro* Evaluation, and Molecular Docking Studies of Novel Pyrazoline Derivatives as Promising Bioactive Molecules

Shivani Sukdev Jadhav *, Pravin Rangnath Dighe, Manoj R Kumbhare

Department of Pharmaceutical Chemistry, S.M.B.T. College of Pharmacy, Dhamangaon, Nashik, Affiliated to Savitribai Phule Pune University, Pune, Maharashtra 422403, India.

Citation S.S. Jadhav, P.R. Dighe, M.R. Kumbhare Synthesis, *In Vitro* Evaluation, and Molecular Docking Studies of Novel Pyrazoline Derivatives as Promising Bioactive Molecules. *J. Pharm. Sci. Comput. Chem.* **2025**, 1 [3], 190-209.

https://doi.org/10.48309/jpscc.2025.538184.1024

Article info:
Submitted: 2025-07-30
Revised: 2025-08-13
Accepted: 2025-08-17
Published: 2025-08-19
ID: JPSCC-2507-1024

Keywords:
Pyrazoline
Molecular docking
Swiss ADME
Biological activity.

ABSTRACT

Pyrazoline derivatives are a promising pharmacophore, as demonstrated by various biological applications. This work relies on computational and spectroscopic methods to synthesize, structurally characterize, and biologically evaluate novel pyrazoline derivatives, synthesizing novel pyrazoline derivatives and evaluating their anti-inflammatory and antioxidant activities using both *in vitro* and *in silico* methods. Pyrazoline derivatives (4a–4e) have been produced by cyclizing chalcones with acetylhydrazine hydrate. The compounds have been analyzed using FTIR, ^{1}H-NMR, ^{13}C-NMR, and mass spectrometry. The hydrogen peroxide scavenging assay has been employed to measure antioxidant activity, while the egg albumin denaturation method has been utilized to assess anti-inflammatory activity. Pharmacokinetic profiling was conducted using Swiss ADME, and PyRx and Discovery Studio were used for molecular docking studies against human transthyretin (1DVX) and LsfA (6POW). Compound 4e showed the highest anti-inflammatory activity (54.12%, IC_{50} = 40.68 µg/ml), while compound 4a exhibited the best antioxidant effect (IC_{50} = 29.86 µg/ml). With docking scores ranging from -6.4 to -7.6 kcal/mol, compound 4b possessed the highest binding affinity (-7.6 kcal/mol). Oral bioavailability increased, in accordance with the Swiss ADME study. These findings suggest that the derived pyrazoline derivatives, especially 4a, 4b, and 4e, possess potent anti-inflammatory and antioxidant properties, making them potential candidates for further therapeutic research.

Introduction

Chalcones are an essential part of intermediates in the synthesis of various bioactive heterocycles. They are made up of a three-carbon chain that connects two aromatic rings with an α, β-unsaturated carbonyl system (1). Acetophenones and aromatic aldehydes can be synthesized through the Claisen–Schmidt condensation process, typically in basic conditions such as ethanol with sodium hydroxide added (2). Chalcones have generated a lot of interest in medicinal chemistry due to their simple structure, ease of functionalization, and wide range of biological activities, including anti-inflammatory, antioxidant, antibacterial, anticancer, and antitubercular properties (3). Pyrazolines are the most significant of the heterocyclic frameworks derived from chalcones. Chalcones usually undergo cyclocondensation with hydrazine or its

**Corresponding Author: Shivani Sukdev Jadhav (jadhavshivanisukdev@gmail.com)*

derivatives to form these nitrogen-containing heterocycles, which have two neighbouring nitrogen atoms, five members, and an endocyclic double bond (4). Specifically, 2-pyrazoline, the most stable tautomeric form, provides a practical scaffold for drug development because it can interact with biological targets through π–π interactions and form hydrogen bonds (5). In this study, substituted chalcones were cyclized with acetyl hydrazine hydrate under reflux conditions using glacial acetic acid to produce a novel series of pyrazoline derivatives (4a–4e). The synthetic approach applied chemical principles by using thin-layer chromatography (TLC) to monitor the reactions and ethanol as a solvent (6). The purity and structural integrity of the generated compounds were confirmed using a variety of spectroscopic techniques: FTIR spectroscopy was used to identify important functional groups, including carbonyl (C=O), nitro (NO_2), and aromatic C=C stretches (7). To elucidate the chemical environment of hydrogen and carbon atoms, ^{1}H-NMR and ^{13}C-NMR spectroscopy were used to confirm the presence of methoxy, hydroxyl, and pyrazoline ring protons (8). The displayed molecular formulas were validated by precise molecular weight measurements obtained using high-resolution mass spectrometry (HRMS) (9). In addition to being structurally defined, these synthetic pyrazoline derivatives were evaluated for their antioxidant and anti-inflammatory activities using *in vitro* tests such as hydrogen peroxide scavenging and egg albumin denaturation (10). Molecular docking studies were carried out using PyRx and Discovery Studio to further investigate the compounds' binding affinities with the anti-inflammatory target protein LsfA (PDB ID: 6P0W) (11) and the antioxidant-related protein transthyretin (PDB ID: 1DVX) (12). These computational techniques showed strong ligand-receptor interactions, and the binding energies matched those of standard drugs such as diclofenac and ascorbic acid (13). Furthermore, the use of Swiss ADME profiling confirmed promising drug-likeness and pharmacokinetic properties in accordance with Lipinski's Rule of Five, which supports their oral bioavailability and therapeutic potential (14). The potential application of pyrazoline derivatives in the synthesis of novel antioxidant and anti-inflammatory medications is highlighted by this comprehensive approach, which combines computational modelling, biological screening, spectroscopic characterization, and synthetic organic chemistry (15).

History

Benzylideneacetophenone, a three-carbon α, β-unsaturated carbonyl system, links two aromatic rings to give chalcones their characteristic structure. The general structure of chalcones is depicted in Figure 1. Their simple structure and variety of biological effects have drawn scientific attention, and they are members of the flavonoid family (16).

Initial Discovery: In the early 19th century, chemists began studying chalcones as they isolated and described a range of natural chemicals from plants (17). Initially discovered in plant pigments, chalcones serve as linkages in the synthesis of isoflavonoids and flavonoids (18).

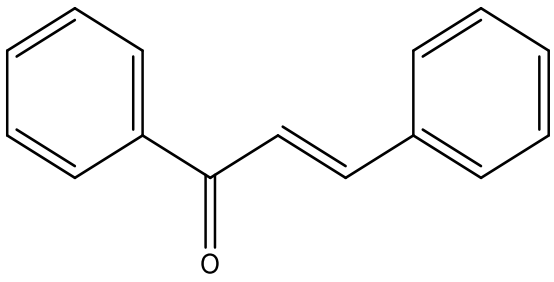


Figure 1: Structure of chalcone

Chemistry: An acetophenone and an aldehyde completed an aldol condensation process to produce the chalcones (19). Aldol condensation is a chemical process in which an enol or an enolate ion reacts with a carbonyl molecule to form β-hydroxyketone, which is subsequently dehydrated to yield a conjugated enone (20).

Overview of Pyrazoline

Recently, there has been a lot of interest in pyrazoline heterocycles due to their diverse pharmacological properties and flexible synthesis methods (21). To enhance the biological effectiveness of pyrazoline derivatives, scientists have focused on developing new synthetic strategies. Pyrazolines have recently been studied in combination with several heterocyclic systems, such as furans, thiophenes, and pyridines (22). These multi-step syntheses aim to convert readily available starting materials into complex pyrazoline derivatives with a greater structural variety and potential biological properties (23). Additionally, the cyclocondensation of chalcones with acetyl hydrazine derivatives is a popular method for pyrazoline scaffold creation, as depicted in Figure 2. The efficiency of this approach in producing compounds with significant pharmacological potential has been extensively researched (24).

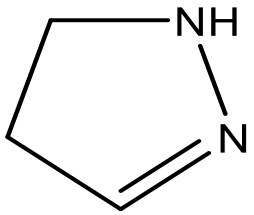


Figure 1: Structure of pyrazoline

Mechanism of Pyrazoline Synthesized from Chalcones

a) Nucleophilic Addition of Hydrazine: A substituted hydrazine derivative, such as acetyl hydrazine, functions as a nucleophile and contributes to the chalcone's α, β-unsaturated carbonyl system (25). In this step, an acetyl hydrazone intermediate is formed by nucleophilically attacking the electrophilic β-carbon of the α, β-unsaturated carbonyl group (C=C–C=O) in the chalcone (26).
b) Intramolecular Cyclization: Acetyl hydrazone, an intermediate, is involved in this process. At this point, the nitrogen atom of acetyl hydrazone attacks the carbonyl carbon to form a five-membered ring. As a result of this reaction, a pyrazoline ring with two nitrogen atoms in the ring structure is produced (27).
c) Protonation and Rearrangement: Protonation and tautomerization of the newly generated pyrazoline intermediate may stabilize the product and create a pyrazoline depending on the substituents on the chalcone and the hydrazine used (28).

Materials and Methods

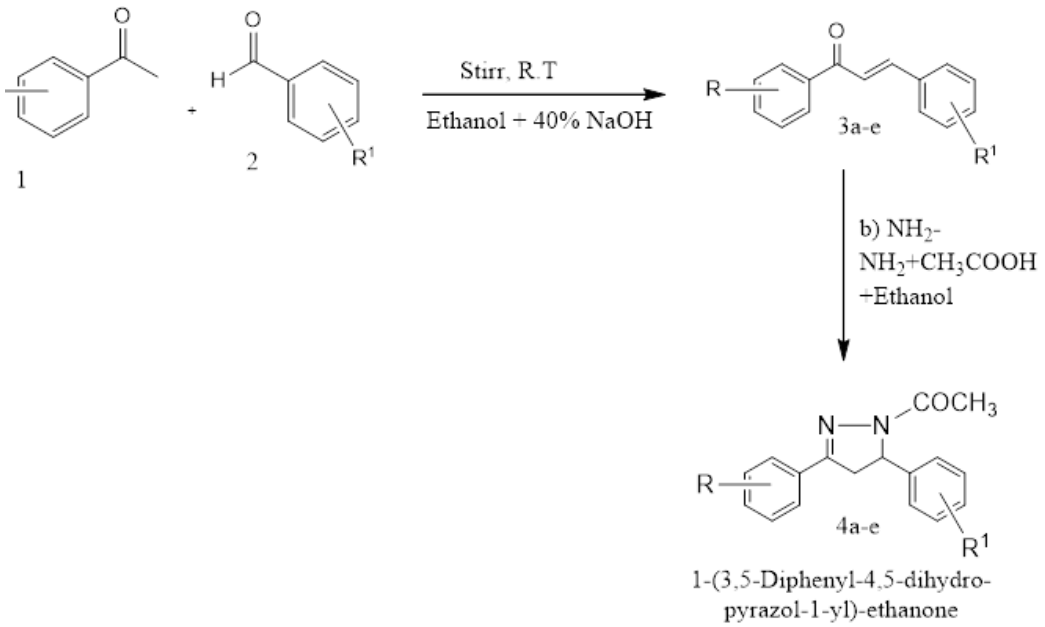


Figure 3: Synthetic pathway

Table 1: Synthesized compound

Comp. code	R	R1
4a	p- NO_2	-OCH_3
4b	p-NO_2	o-OH
4c	p-CH_3	2,4-dichloro
4d	p- CH_3	2,6-dichloro
4e	p-NO_2	-H

The structures and substituents of the synthesized pyrazoline derivatives (4a–4e) are summarized in Table 1.

Procedure for Synthesis of A, B-Unsaturated Ketone (3a-E)

3–5 ml of ethanol dissolved 1 mmol of substituted methoxy benzaldehyde and 1 mmol of p-hydroxy acetophenone. Following the addition of a catalytic quantity of NaOH, the reaction mixture was stirred for approximately 8 hours at room temperature. Under UV light, the reaction was observed using Merck pre-coated TLC plates 60F-254, with n-hexane and ethyl acetate (8:2) serving as the solvent solution. At the end of the reaction, the precipitate sank to the bottom of the reaction mixture, which was then placed in ice-cold water. After that, ethanol was used to filter, dry, and recrystallize it (29), as illustrated in Figure 3.

Procedure for Synthesis of (4a-e)

In a round-bottom flask, a chalcone (1 mmol) in ethanol (5 ml) was mixed with glacial acetic acid (1 mmol) and hydrazine hydrate (1 mmol). The reaction mixture was heated to 80 °C with reflux for six hours in a water bath. The reaction was monitored using Merck precoated aluminium TLC plates 60F-254, and the solvent solution used to visualize the outcome under UV light was n-hexane and ethyl acetate. The reaction liquid was placed in ice-cold water once the reaction was complete, and the precipitate was filtered, dried, and

recrystallized with ethanol (30). The synthetic pathway of the pyrazoline derivatives is shown in Figure 3.

Biological Evaluation

Anti-Inflammatory Activity: in Vitro egg Albumin Method

The purpose of the egg albumin denaturation assay is to examine whether any substances may prevent the denaturation or structural alteration of egg albumin under particular circumstances. Heat, pH variations, or denaturing chemicals cause denaturation, or the loss of the protein's biological activity, in this experiment. The experiment uses the model protein egg albumin to evaluate how chemicals or medications may inhibit or prevent denaturation, indicating anti-inflammatory properties. The idea is that anti-inflammatory substances could stabilize protein structures, preventing denaturation, which is linked to tissue damage and inflammation. An effective reduction in the denaturation of egg albumin in this assay suggests possible anti-inflammatory qualities. Through the simultaneous inhibition of the COX enzyme and protein denaturation, which is partially associated with inflammation, NSAIDs stop this process (31).

Procedure

2 ml of the produced chemical at different concentrations, 2.8 ml of phosphate buffered saline (pH 6.4), and 0.2 ml of egg albumin (from a fresh hen's egg) make up the reaction mixture (5 ml). A similar amount of double-distilled water was utilized as a control. The mixtures were incubated at 37±2 ºC for 15 minutes, and then heated to 70 ºC for 5 minutes. Their absorbance at 660 nm was measured using the vehicle as a blank once it had cooled. Diclofenac was used as the reference drug and treated similarly in order to calculate absorbance. The % inhibition of protein denaturation was calculated using the following formula (32).

$$\text{Percentage Inhibition (\%)} = \frac{(\text{Ao} - \text{As})}{\text{Ao}} \times 100$$

Where, As is the absorbance of Diclofenac or synthesized test compounds and Ao is the absorbance of the blank.

Antioxidant Activity: Hydrogen Peroxide Scavenging Assay

Hydrogen peroxide scavenging is a common technique for determining hydrogen peroxide. A compound's H_2O_2 scavenging activity is measured by assessing the H_2O_2 disappearance at 230 nm (33). Peroxide ions are formed by several oxidase enzymes. The present investigation aims to confirm the hypothesis that the reduction of hydrogen peroxide to hydroxide ions (OH-) causes damage to biological systems. With this approach, hydrogen peroxide is incubated with an antioxidant-containing molecule, and the reduction or degradation of hydrogen peroxide at 230 nm is assessed using spectrometric techniques (34). Mechanism for antioxidant activity by H_2O_2 model (32) is given in the formula given below:

$$2H_2O_2 \xrightarrow{\text{e- from antioxidant}} 2H_2O + O_2$$

Procedure

A phosphate buffer with a pH of 7.4 was used to prepare 40 mM of H_2O_2. The sample was produced in a variety of concentrations (20, 40, 60, 80, and 100). Absorption spectrophotometry at 230 nm was used to measure the H_2O_2 concentration. This was accomplished by adding 1 mL increments of the synthesized product (0.6 mL, 40 mM) to the H_2O_2 solution. Ten minutes later, the absorption of H_2O_2 at 230 nm was utilized to measure a reference solution that contained phosphate buffer but did not contain H_2O_2. The following methodology was employed to ascertain the hydrogen peroxide inhibition (35).

$$\text{Percentage Inhibition (\%)} = \frac{(\text{Ao} - \text{As})}{\text{Ao}} \times 100$$

Where, As is the absorbance of ascorbic acid or synthesized test compounds, and Ao is the absorbance of the blank.

Molecular docking study

In silico study

An *in silico* assessment of the chemical in question was carried out using Swiss ADME software. Mebendazole and Ibipinabant are used as reference standards (36).

Molecular Docking

PyRx Virtual Screening Tools were used for molecular docking of the molecule. The RCSB Protein Data Repository was used to retrieve the X-ray crystallography. The protein was prepared using AutoDock Tools, and the docking was visualized using Discovery Studio 2021 (37).

Procedure for Molecular Docking

Molecular docking was carried out using a range of software applications, including as PyRx, PyMOL, Discovery Studio, PDB, and ChemDraw. The three main older apps are PyRx, PyMOL, and Discovery Studio. The molecular docking phase is being completed by them (38).

a. Make a ChemDraw that shows the chemical structure of the drug.

b. Protein Selection: Based on biological activity and pertinent data, proteins are selected from the PDB and stored as PDB files. The protein structure retrieved from the PDB database is shown in Figure 4.

Discovery Studio

The ability to bind particular proteins and analyze two-dimensional ligand-protein interactions is thus made possible. Following the collection of protein data banks and protein crystal structures, the best medications were subjected to molecular docking studies using the PyRx and PyMOL tools. The receptor was constructed using the PyMOL algorithm, which substituted polar hydrogen atoms for ligands and water molecules. The PyRx tool is used to create the drug-protein complex., The docking score was determined in kcal/mol. The Discovery Studio Visualizer was used to analyse each ligand-protein interaction. The 2D and 3D interactions are visualized in Figure 7 (39).

PyRx

A ligand-protein interaction may be involved in this application, as binding affinity was noted. Water molecules removed during protein preparation are illustrated in Figure 5.

PyMOL

In PDB format, protein-ligand interaction showing the docking pose of ligand and protein is presented in Figure 6.

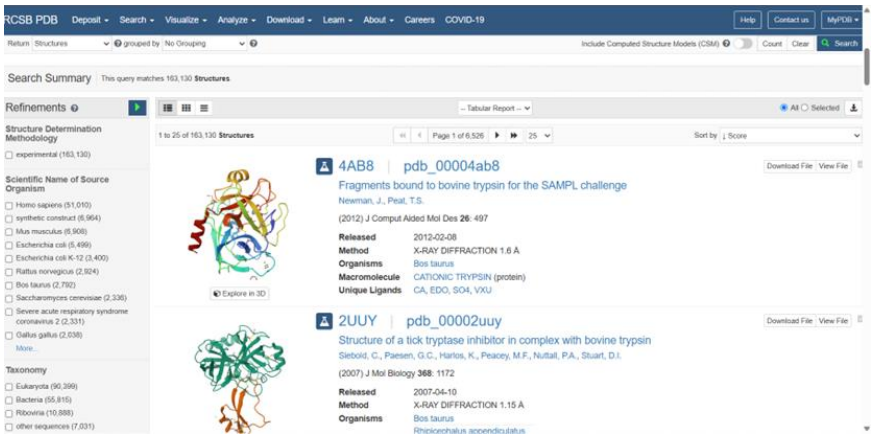


Figure 4: Downloaded protein in PDB

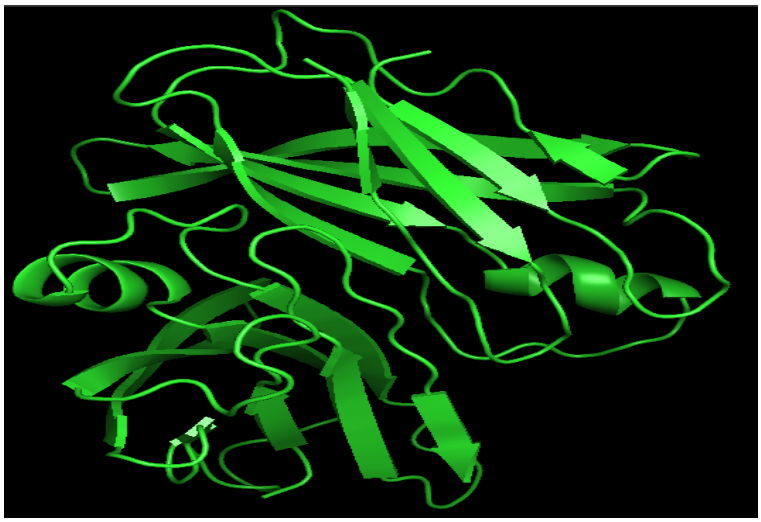


Figure 2: 3D view of the purified protein enzyme.

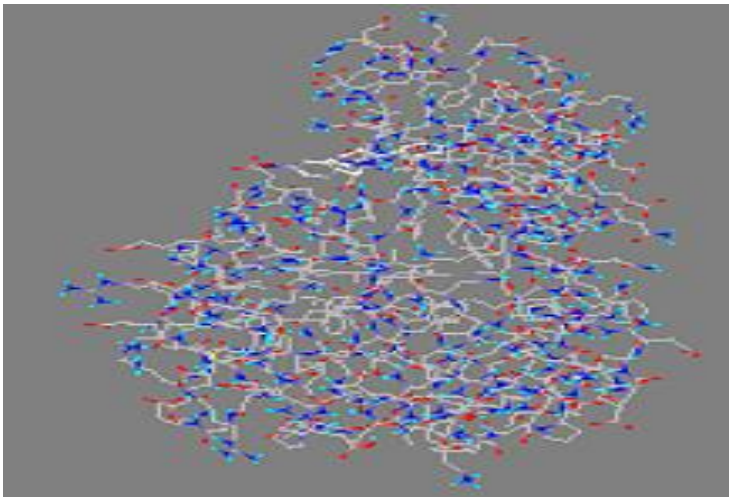


Figure 3: Protein and ligand bind

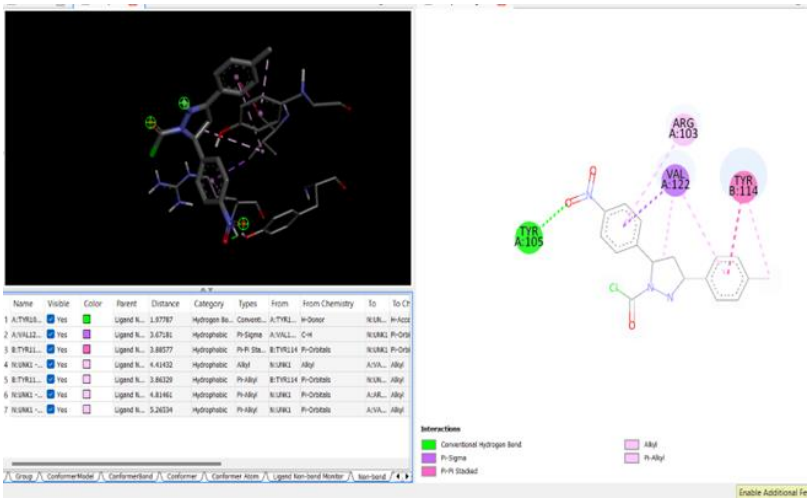


Figure 7: 2D and 3D structures

Results and Discussion

4a: *1-[5-(2-Methoxy-phenyl)-3-(4-nitro-phenyl)-4,5-dihydro-pyrazol-1-yl]-ethanone*
M.F: $C_{18}H_{17}N_3O_4$, M.wt: 339.35, Yield: 78%, M.P.: 180-182 °C, Rf: 0.54, FT-IR: 2834.90 (SP^3C-H str), 3045.89 (SP^2C-H str), 1646.52 (C=O str), 1593.91, 1494.79 (Ar C=C Str), 1241.43 (NO_2 str), and 1124.43 (C-O str). ^{1}H-NMR: ($CDCl_3$-500MHz): 2H of CH_2, d (2.083-2.118), 3H of OCH_3, s (3.836), 1H of N-CH, t (3.748-3.773), 3H of $COCH_3$, s (3.033), and 8H of Ar-H, m (6.669-6.918). ^{13}C-NMR: 112.65-143.39 (19C of Ar-C, m), 76.760 (1Cof N-CH), and 77.26 (1C of CH-CH_2).MS: (m/z)- Mol.wt: 339.35, Molecular ion peak: 339.17.

4b: *1-[5-(2-Hydroxy-phenyl)-3-(4-nitro-phenyl)-4,5-dihydro-pyrazol-1-yl]-ethanone*
M.F: $C_{17}H_{15}N_3O_4$, M. wt: 325.32, Yield: 84 %, M.P.: 187-190 °C, Rf: 0.60, FT-IR: 3284.12 (O-H str), 3022.87 (SP^2C-H str), 2850, 2960 (SP^3C-H str), 1650.74 (C=O str), 1493.14,1595.68 (Ar C=C str), 1372.53 (NO_2str), and 1236.48(C-O str). ^{1}H-NMR: ($CDCl_3$-500MHz): 4.654, s (1H of NH) 2.944-2.959, d (2Hof CH_2), and 4.066-4.291, t (1Hof N-CH). ^{13}C-NMR: 43.916 **(**1C of CH_3), 112.432-127.563 (2**C** of Ar -C, m),160.01 (1C of C=O), 55.26 (1C of N-CH),63.900 (1H of CH-CH_2). MS: (m/z)- Mol.wt: 325.32, Molecular ion peak: 325.39.

4c: *1-[5-(2,4-Dichloro-phenyl)-3-(4-nitro-phenyl)-4,5-dihydro-pyrazol-1-yl]-ethanone*
M.F: $C_{18}H_{17}Cl_2N_3O_3$, M. wt: 394.25, Yield: 94 %, M.P.: 177-179 °C, Rf 0.54, FT-IR: 2946.38 (SP^3C-H str), 3145.56 (SP^2C-H str), 1697.48 (C=O str), 1580.20, 1518.81(Ar C=C str), 1310.23 (NO_2 str), and 627.33(C-Cl str).

4d: *1-[5-(2,6-Dichloro-phenyl)-3-(4-nitro-phenyl)-4,5-dihydro-pyrazol-1-yl]-ethanone*
M.F: $C_{17}H_{13}Cl_2N_3O_3$, M. wt: 378.21, Yield: 76 %, M.P.: 192-194 ° C, Rf: 0.53, FT-IR: 2857.17 (SP^3 C-H str), 3047.72 (SP^2 C-H str), 1687.92 (C=O str), 1595.52, 1495.01 (Ar C=C str), 1343.84 (NO_2 str), and 687.62 (C-Cl str).

4e: *3-[2-Acetyl-5-(4-nitro-phenyl)-3,4-dihydro-2H-pyrazol-3-yl]-benzaldehyde*
M.F: $C_{18}H_{15}N_3O_4$, M. wt:337.33, Yield: 88 %, M.P.: 184-186 °C, Rf: 0.58, FT-IR: 3022.84 (SP^2C-H str), 2850.80 (SP^3C-H str), 1594.60,1493.03 (Ar C=C str), and 688.22 (C-Cl str).

The docking interactions for anti-inflammatory activity are detailed in Table 2.

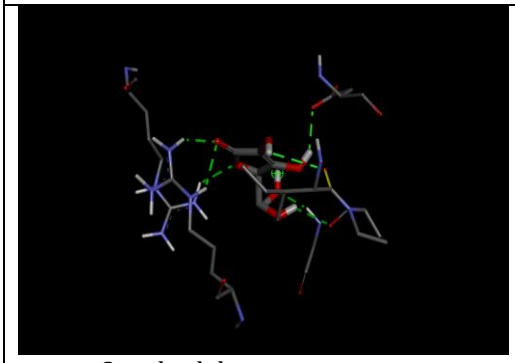
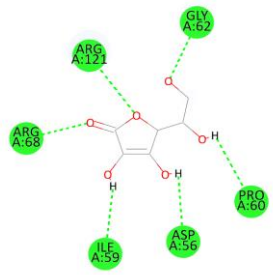
Table 1: Molecular docking study of pyrazoline derivatives for anti-inflammatory activity

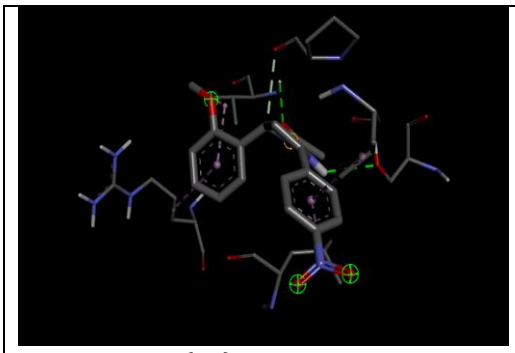
PDB ID: LsfA from P. *aeruginosa* (**6POW**)					
Bonds between compound atoms and residues from active sites					
Compound	**Mol. dock score (kcal/ mol)**	**Receptor involved Residue**	**Category**	**Type**	**Distance (Å)**
Std. drug (Diclofenac sodium)	-7.9	N: UNK1	H-Bond	Conventional H-Bond	2.53727
		N: UNK1	H-Bond	Conventional H-Bond	2.38165
		A: ASP99	H-Bond	Conventional H-Bond	2.06801
		A: VAL122	Hydrophobic	Pi-Alkyl	4.99597
		N: UNK1	Hydrophobic	Pi-Alkyl	4.65792
4a	-7.1	A: ARG21	H-Bond	Conventional H-Bond	2.20054
		A: ILE26	H-Bond	Conventional H-Bond	1.91155
		N: UNK1	H-Bond	Conventional H-Bond	3.06266
		N: UNK1	H-Bond	Conventional H-Bond	2.36328
		A: TYR78	H-Bond	Carbon H-Bond	3.19844
		A: LYS48	Electrostatic	Pi-Cation	4.44874
		A: ASN27	H-Bond	Pi-Donor H-Bond	3.13994

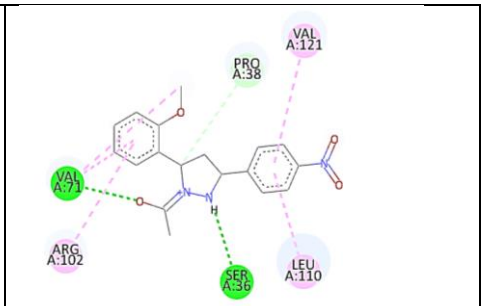
		A: ILE26	Hydrophobic	Pi-Sigma	3.91682
4b	-7.6	A: THR96	H-Bond	Conventional H-Bond	2.33973
		A: ARG103	H-Bond	Conventional H-Bond	2.06361
		A: ARG103	H-Bond	Conventional H-Bond	2.22948
		N: UNK1	H-Bond	Conventional H-Bond	2.96457
		N: UNK1	H-Bond	Conventional H-Bond	2.12581
		A: THR96	H-Bond	Carbon H-Bond	3.12624
4c	-6.8	A: ASN98	H-Bond	Conventional H-Bond	2.75866
		N: UNK1	H-Bond; Halogen	Carbon H-Bond; Halogen (Cl, Br, I)	2.96612
		A: VAL121	H-Bond	Pi-Donor H-Bond	3.39052
		A: VAL122	Hydrophobic	Pi-Sigma	3.87373
		B: TYR114	Hydrophobic	Pi-Pi T-shaped	4.74559
		N: UNK1: Cl	Hydrophobic	Alkyl	5.06954
		N: UNK1	Hydrophobic	Pi-Alkyl	3.81886
		N: UNK1	Hydrophobic	Pi-Alkyl	4.83122
4d	-6.4	A: LYS70	H-Bond; Electrostatic	Pi-Cation; Pi-Donor Hydrogen Bond	2.76219
		B: LYS70	Electrostatic	Pi-Cation	3.64368
		A: PHE33	Hydrophobic	Pi-Pi T-shaped	5.0104
		A: TRP41	Hydrophobic	Pi-Pi T-shaped	5.24714
		B: TRP41	Hydrophobic	Pi-Pi T-shaped	5.10358
4e	-7.3	A: ASN98	H-Bond	Conventional H-Bond	2.7035
		A: ASP99	H-Bond	Conventional H-Bond	2.78686
		A: TYR105	H-Bond	Conventional H-Bond	2.02407
		A: VAL121	H-Bond	Carbon H-Bond	3.49117
		B: TYR114	Hydrophobic	Pi-Pi Stacked	4.2522
		N: UNK1	Hydrophobic	Pi-Alkyl	4.78965
		N: UNK1	Hydrophobic	Pi-Alkyl	4.54251
		N: UNK1	Hydrophobic	Pi-Alkyl	5.41146

The 3D and 2D structures of the synthesized compounds are presented in Table 3.

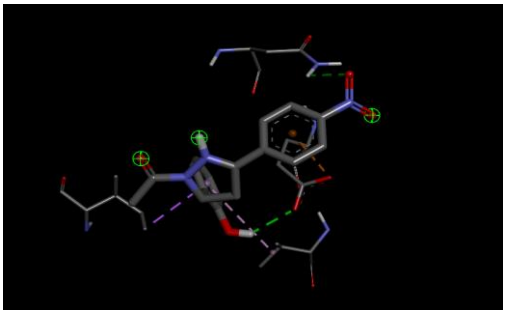
Table 2: 3D and 2D structures of synthesized compound

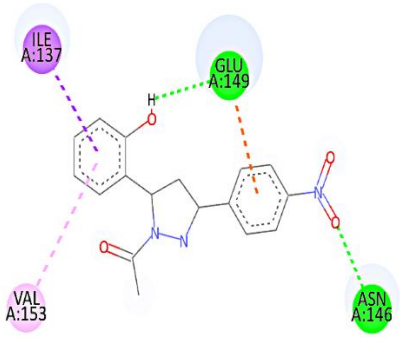
3D-Structure	2D-Structure
 Standard drug	



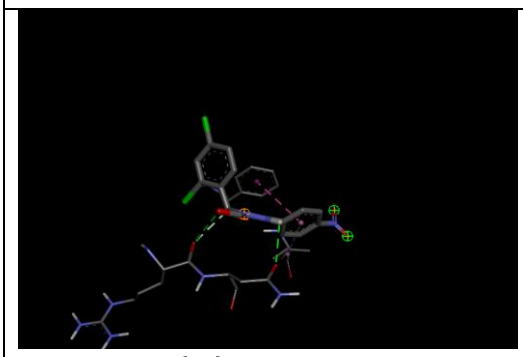

VAL A:121
PRO A:38
VAL A:71
ARG A:102
SER A:36
LEU A:110

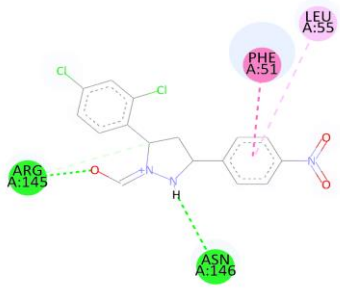
(4a)



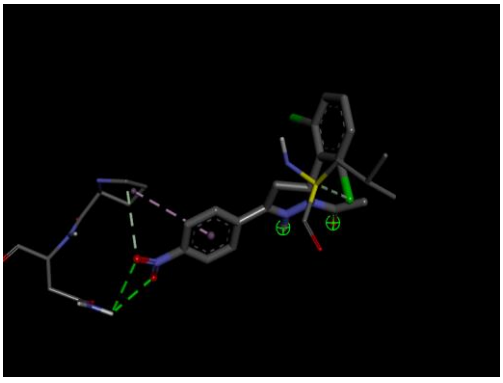

ILE A:137
GLU A:149
VAL A:153
ASN A:146

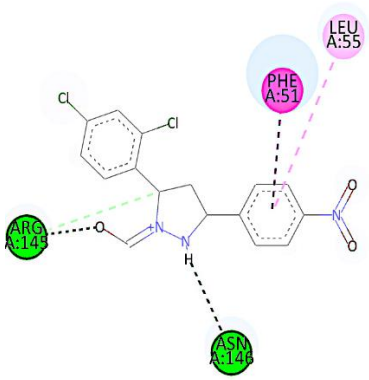
(4b)



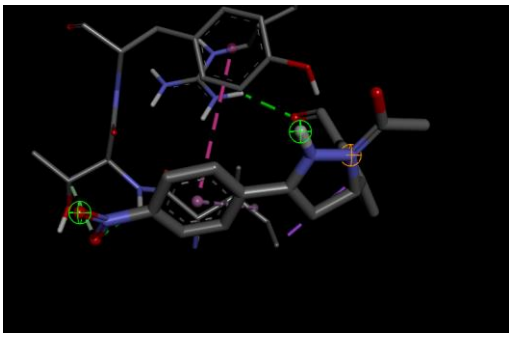

LEU A:55
PHE A:51
ARG A:145
ASN A:146

(4c)




LEU A:55
PHE A:51
ARG A:145
ASN A:146

(4d)



(4e)

The *in vitro* anti-inflammatory activity of pyrazoline derivative is summarized in Table 4.

Table 3: *In vitro* anti-inflammatory activity of pyrazoline derivatives

Comp. code	Conc.(µg/ml)	% inhibition	Standard deviation ±IC_{50}
Std	20	40.68	
	40	40.83	
	60	41.18	4.945±55.40
	80	42.29	
	100	42.82	
4a	20	48.03	
	40	49.70	
	60	50.24	2.52±51.11
	80	51.36	
	100	51.91	
4b	20	45.12	
	40	46.75	
	60	48.09	3.28±53.00
	80	51.56	
	100	52.94	
4c	20	45.19	
	40	46.93	
	60	48.06	2.36±46.71
	80	51.37	
	100	53.45	
4d	20	42.61	
	40	45.23	
	60	48.59	2.43±48.85
	80	51.78	
	100	53.25	
4e	20	46.16	
	40	49.95	
	60	51.43	1.24±40.68
	80	53.78	
	100	54.12	

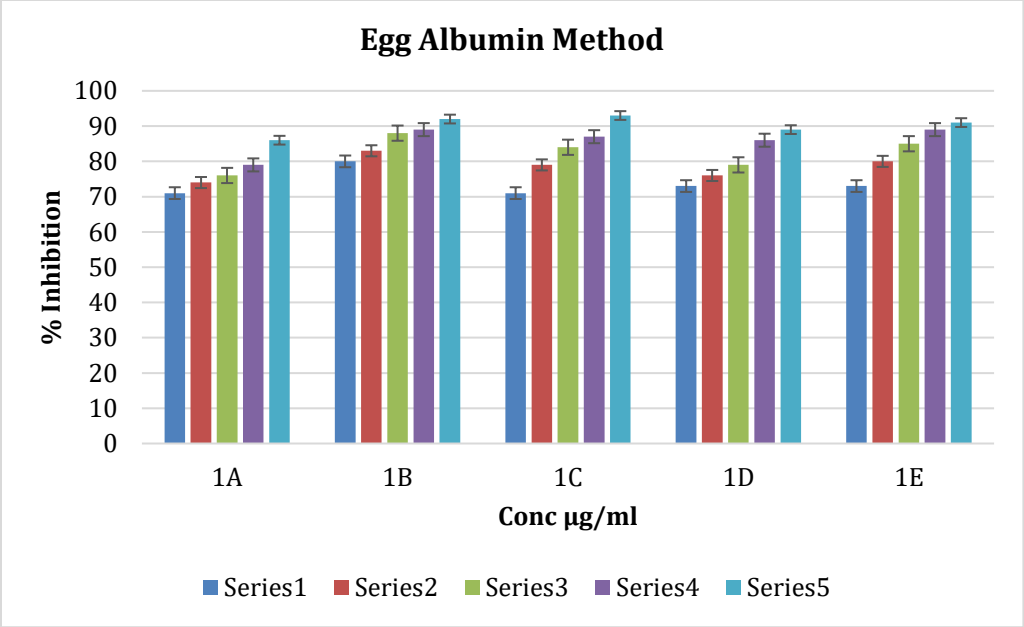


Figure 4: *In vitro* anti-inflammatory activity by egg albumin method

Table 4: Molecular docking study of pyrazoline derivatives for anti-oxidant activity

PDB ID: Crystal Structure of Human Transthyretin **(1DVX)**

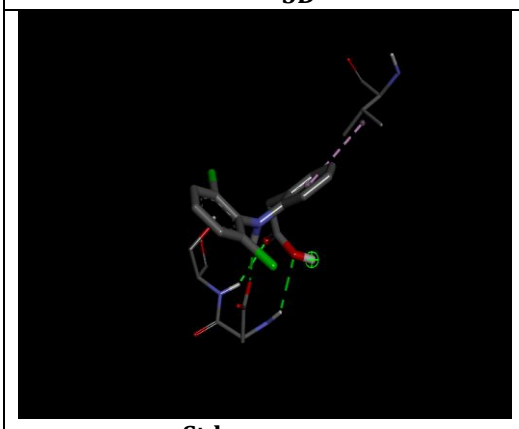
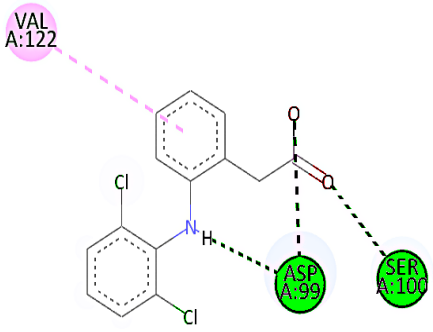
Bonds between compound atoms and residues from active sites

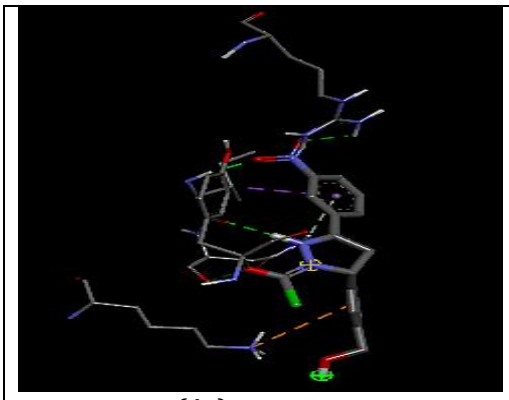
Compound	Mol dock score (Kcal/ mol)	Receptor involved Residue	Category	Type	Distance (Å)
Std drug (Ascorbic acid)	-7.9	N: UNK1	H-Bond	Conventional H-Bond	2.53727
		N: UNK1	H-Bond	Conventional H-Bond	2.38165
		A: ASP99	H-Bond	Conventional H-Bond	2.06801
		A: VAL122	Hydrophobic	Pi-Alkyl	4.99597
4a	-7.1	A: ARG21	H-Bond	Conventional H-Bond	2.20054
		A: ILE26	H-Bond	Conventional H-Bond	1.91155
		N: UNK1	H-Bond	Conventional H-Bond	3.06266
		N: UNK1	H-Bond	Conventional H-Bond	2.36328
		A: TYR78	H-Bond	Carbon H-Bond	3.19844
		A: LYS48	Electrostatic	Pi-Cation	4.44874
		A: ASN27	H-Bond	Pi-Donor H-Bond	3.13994
		A: ILE26	Hydrophobic	Pi-Sigma	3.91682
4b	-7.6	A: THR96	H-Bond	Conventional H-Bond	2.33973
		A: ARG103	H-Bond	Conventional H-Bond	2.06361
		A: ARG103	H-Bond	Conventional H-Bond	2.22948
		N: UNK1	H-Bond	Conventional H-Bond	2.96457
		N: UNK1	H-Bond	Conventional H-Bond	2.12581
		A: THR96	H-Bond	Carbon H-Bond	3.12624
4c	-6.8	A: ASN98	H-Bond	Conventional H-Bond	2.75866

		N: UNK1	H-Bond; Halogen	Carbon H-Bond; Halogen (Cl, Br, I)	2.96612
		A: VAL121	H-Bond	Pi-Donor H-Bond	3.39052
		A: VAL122	Hydrophobic	Pi-Sigma	3.87373
		B: TYR114	Hydrophobic	Pi-Pi T-shaped	4.74559
		N: UNK1: Cl	Hydrophobic	Alkyl	5.06954
		N: UNK1	Hydrophobic	Pi-Alkyl	3.81886
		N: UNK1	Hydrophobic	Pi-Alkyl	4.83122
4d	-6.4	A: LYS70	H-Bond; Electrostatic	Pi-Cation; Pi-Donor Hydrogen Bond	2.76219
		B: LYS70	Electrostatic	Pi-Cation	3.64368
		A: PHE33	Hydrophobic	Pi-Pi T-shaped	5.0104
		A: TRP41	Hydrophobic	Pi-Pi T-shaped	5.24714
		B: TRP41	Hydrophobic	Pi-Pi T-shaped	5.10358
4e	-7.3	A: ASN98	H-Bond	Conventional H-Bond	2.7035
		A: ASP99	H-Bond	Conventional H-Bond	2.78686
		A: TYR105	H-Bond	Conventional H-Bond	2.02407
		A: VAL121	H-Bond	Carbon H-Bond	3.49117
		B: TYR114	Hydrophobic	Pi-Pi Stacked	4.2522
		N: UNK1	Hydrophobic	Pi-Alkyl	4.78965
		N: UNK1	Hydrophobic	Pi-Alkyl	4.54251
		N: UNK1	Hydrophobic	Pi-Alkyl	5.41146

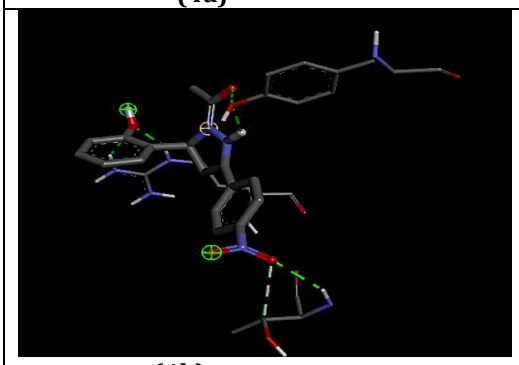
The docking interactions of the synthesized derivatives with human transthyretin (PDB ID: 1DVX) are detailed in Table 5.

Table 5: 2D and 3D formations of the synthesized compounds for protein 1DVX

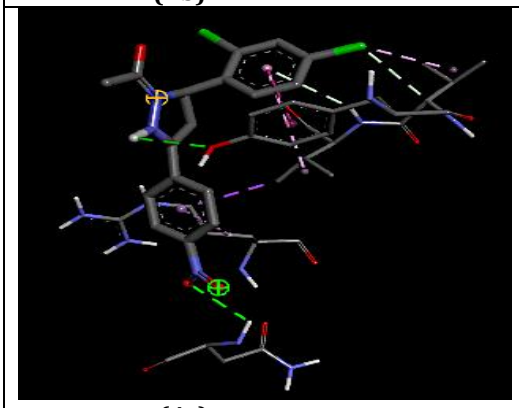
3D	2D
	
Std	


LYS
A:48
Cl
N
N
H
O
O
N
O
ASN
A:27
ILE
A:26
ARG
A:21
TYR
A:78

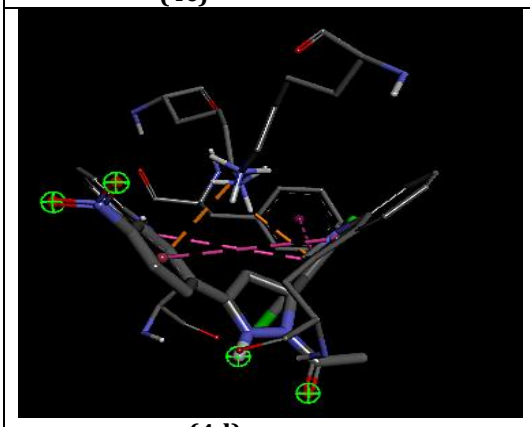
(4a)


O
N
O
THR
A:96
N
N
H
O
O
TYR
B:114
ARG
A:103

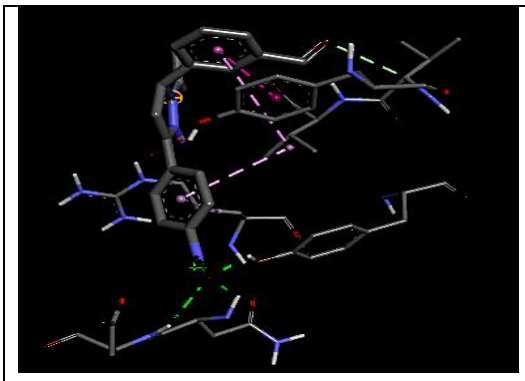
(4b)


TYR
B:114
ASN
A:98
H
N
O
O
N
O
VAL
A:121
Cl
Cl
VAL
A:122
ARG
A:103

(4c)


TRP
B:41
LYS
B:70
TRP
A:41
O
N
O
Cl
PHE
A:33
Cl
LYS
A:70

(4d)



(4e)

Visualizations of protein-ligand binding interactions with the antioxidant target (1DVX) are presented in Table 6.

Table 7: Hydrogen Peroxide scavenging activity

Comp. code	Conc.(µg/ml)	% inhibition	Standard deviation ±IC_{50}
Std	20	48.37	
	40	50.83	
	60	49.37	4.98±58.25
	80	52.18	
	100	53.21	
4a	20	48.91	
	40	51.12	
	60	51.60	1.52±29.86
	80	54.68	
	100	54.82	
4b	20	46.83	
	40	50.83	
	60	50.72	2.917±35.85
	80	51.31	
	100	52.83	
4c	20	49.09	
	40	50.83	
	60	50.76	3.437±40.46
	80	51.35	
	100	52.80	
4d	20	48.81	
	40	50.50	
	60	50.88	1.40±34.08
	80	51.92	
	100	52.40	
4e	20	46.54	
	40	47.83	
	60	49.80	3.41±52.21
	80	51.57	
	100	52.23	

The quantitative antioxidant activity results, including percentage inhibition and IC_{50} values, are compiled in Table 7.

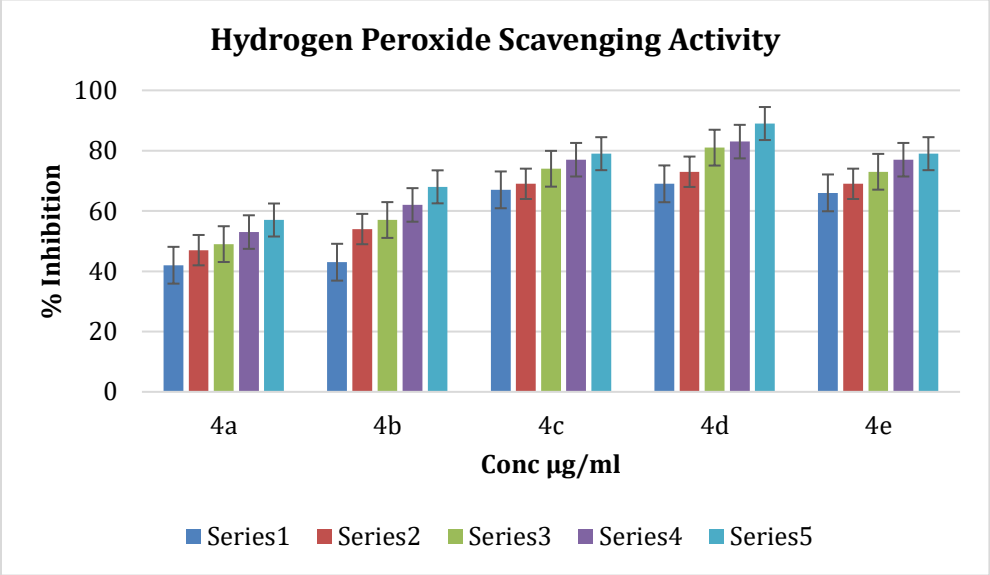


Figure 9: Hydrogen peroxide scavenging activity

The hydrogen peroxide scavenging activity of the compounds is graphically shown in Figure 9.

Table 6: Pharmacokinetics, bioavailability, and medicinal chemistry for derived and standard compounds

Compound	Pharmacokinetics			Bioavailability		
	GI absorption	BBB Permeant	P-gp substrate	Score	Pains	Leadlikness
4a	High	Yes	No	0.55	-	2
4b	High	No	No	0.55	-	2
4c	Low	No	No	0.55	-	1
4d	High	No	No	0.55	-	1
4e	High	No	No	0.55	-	2
STD	High	No	No	056	-	1

Table 7: Veber's Rule and Lipinski's Rule of 5 for derived and standard compounds

Compound	Lipinski's Rule of 5				Veber's Rule		
	Log P	Mol. Wt. (g/mol)	H-bond Acceptor	H-bond Donor	Lipinski	Rotatable	TPSA (Å²)
4a	2.47	339.35	3	0	Yes	4	61.42
4b	2.79	325.32	1	1	Yes	2	56.34
4c	1.83	394.25	2	3	Yes	3	95.52
4d	1.48	378.21	4	2	Yes	2	87.45
4e	1.53	337.33	3	1	Yes	3	67.52
STD	0.31	176.12	6	4	Yes	2	107.22

The pharmacokinetics and bioavailability parameters are listed in Table 8, and compliance with Lipinski's and Veber's rules is shown in Table 9.

The boiled egg plot illustrating BBB permeability and GI absorption is presented in Figure 10.

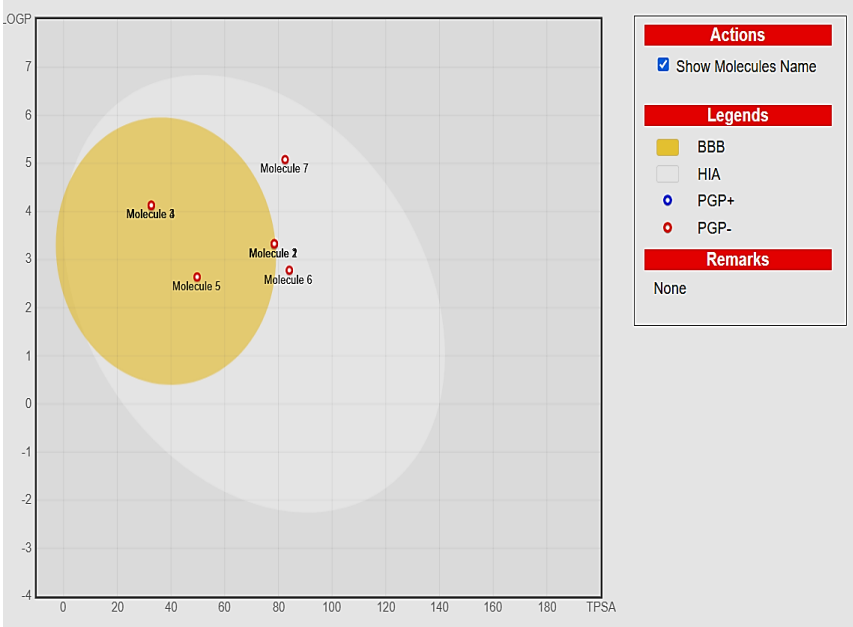


Figure 5: Boiled egg representation of pyrazoline derivatives with standard drug Mebendazole and Ibipinabant

The five pyrazoline derivatives (4a–4e), presented in Table 1, were developed by employing acetyl hydrazine hydrate to create substituted chalcones. The compounds were characterized by means of TLC, IR, ^{1}H-NMR, ^{13}C-NMR, and mass spectrometry.

Molecular Docking

Additionally, it has anti-inflammatory activity against *P. aeruginosa* LsfA (6POW), as shown in (Table 4). In terms of antioxidant activity, it was against human transthyretin (1DVX), as shown in Table 5. Compound 4b had the highest docking score (-7.6 kcal/mol), which was comparable to that of the standard medication diclofenac (-7.9).

In vitro Anti-Inflammatory Activity

In vitro anti-inflammatory *a*ctivity was measured by egg albumin *m*ethod, as demonstrated in Figure 8. Compound 4e showed the strongest inhibition at 100 µg/ml (54.12%), better than standard diclofenac (42.82%). IC_{50} values ranged from 40.68 to 53.00 µg/ml.

In vitro Antioxidant Activity

H_2O_2 scavenging was used for measurement with an IC_{50} of 29.86 µg/ml, as shown in Figure 9. Compound 4a exhibited the highest activity, exceeding ascorbic acid (58.25 µg/ml) by a substantial amount.

The potent interactions with important amino acid residues in the active regions of anti-inflammatory and antioxidant target proteins were identified by molecular docking, and the synthesized derivatives indicated good structural consistency, as shown in Table 6, confirmed by spectroscopy. When compared to the standards, derivatives 4a, 4b, and 4e notably exhibited greater inhibition in both biological investigations. The Swiss ADME analysis results demonstrated that the compounds correspond to Lipinski's and Veber's rules, as shown in Table 9, indicating good oral bioavailability and drug-likeness which is presented in Figure 10. The strong correlation between the docking scores and *in vitro* performance indicates that these compounds may operate through two different mechanisms: free radical scavenging and enzyme inhibition.

Conclusion

It has been shown how to successfully synthesize and structurally characterize a

number of novel pyrazoline derivatives (4a–4e) using mass spectrometry, FTIR, and NMR. While the other compounds showed required antioxidant and anti-inflammatory properties *in vitro*, compounds 4a, 4b, and 4e exhibited highly potent biological potential. Molecular docking studies that showed strong binding affinities to significant proteins connected to inflammation and oxidative stress, confirmed the observed biological activity. Additionally, the Swiss ADME research has identified important pharmacokinetic features, including good oral bioavailability. These results suggest that the synthesized pyrazoline derivatives are promising compounds for further study and development as pharmaceuticals to treat inflammation and diseases linked to oxidative stress. According to these results, the produced pyrazoline derivatives show potential for further research and development as medications to treat oxidative stress-related illnesses and inflammation.

Acknowledgements

The authors are thankful to SMBT College of Pharmacy, for providing the necessary facilities to conduct this research work.

Conflict of Interest

No conflicts of interest were declared by the authors in this work.

Funding

None.

ORCID

Shivani Sukdev Jadhav
https://orcid.org/0009-0004-9369-6007
Pravin Rangnath Dighe
https://orcid.org/0000-0003-0929-0406
Manoj R Kumbhare
https://orcid.org/0000-0002-8906-9578

Reference

[1] Elkanzi, N.A., Hrichi, H., Alolayan, R.A., Derafa, W., Zahou, F.M., Bakr, R.B. Synthesis of chalcones derivatives and their biological activities: a review. *ACS omega*, **2022**, 7(32), 27769-27786.

[2] Wadje SS, Ahmad R, Bamne AS, Ghume NP, Pooja M, Shaikh SK, et al. Synthesis of α , β - unsaturated carbonyl compound and their pharmacological activities. 2024;2(4):757–64.

[3] Sharma, P., Malhi, D.S., Sohal, H.S. Biological potencies of chalcones in medicinal chemistry. *Materials Today: Proceedings*, **2022**, 68, 899-904.

[4] Yadav, C.S., Azad, I., Khan, A.R., Nasibullah, M., Ahmad, N., Hansda, D., Lohani, M.B. Recent advances in the synthesis of pyrazoline derivatives from chalcones as potent pharmacological agents: A comprehensive review. *Results in Chemistry*, **2024**, 7(101326.

[5] Matiadis, D. Strategies and Methods for the Synthesis of 2-Pyrazolines: Recent Developments (2012–2022). *Advanced Synthesis & Catalysis*, **2023**, 365(12), 1934-1969.

[6] North, J., Saari-Nordhaus, R., Doddridge, G., Seefeldt, M., Young, D.A., Liu, Y. Non-destructive Raman Method Development for Quantifying Active Pharmaceutical Ingredient in an Oral Suspension Through Plastic Dosing Syringes. *AAPS PharmSciTech*, **2024**, 25(4), 76.

[7] Gong, Y., Chen, X., Wu, W. Application of fourier transform infrared (FTIR) spectroscopy in sample preparation: Material characterization and mechanism investigation. *Advances in Sample Preparation*, **2024**, 11(100122.

[8] Gunawan, R., Nandiyanto, A.B.D. How to read and interpret 1H-NMR and 13C-NMR spectrums. *Indonesian Journal of Science and Technology*, **2021**, 6(2), 267-298.

[9] Kozlowski, M.C., Correa Otero, G., Zhang, S. On the Integrity of Accurate Mass Measurement Data in Compound Characterization. *Organic Letters*, **2025**, 27(1), 1-3.

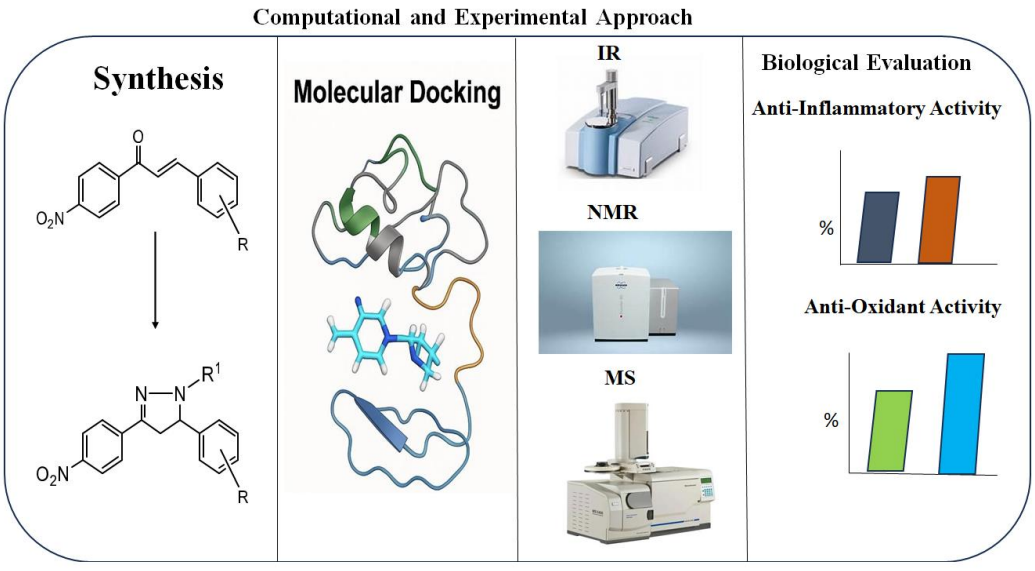
[10] Hassan SY. Synthesis and biological activity of some new pyrazoline and pyrimidine derivatives. *Journal of Brazilian Chemical Society,* **2011,** 22(7), 1286-1298.

[11] Ayodele, P.F., Bamigbade, A., Bamigbade, O.O., Adeniyi, I.A., Tachin, E.S., Seweje, A.J., Farohunbi, S.T. Illustrated procedure to perform molecular docking using PyRx and Biovia discovery studio visualizer: a case study

of 10kt with atropine. *Progress in Drug Discovery & Biomedical Science*, **2023**, 6(1).
[12] Klabunde, T., Petrassi, H.M., Oza, V.B., Kelly, J.W., Sacchettini, J.C. Rational design of potent human transthyretin amyloid disease inhibitors. *Nature Structural Biology*, **2000**, 7, 312-321.
[13] Pieroni, M., Madeddu, F., Di Martino, J., Arcieri, M., Parisi, V., Bottoni, P., Castrignanò, T. MD–ligand–receptor: a high-performance computing tool for characterizing ligand–receptor binding interactions in molecular dynamics trajectories. *International Journal of Molecular Sciences*, **2023**, 24(14), 11671.
[14] Daina, A., Michielin, O., Zoete, V. SwissADME: a free web tool to evaluate pharmacokinetics, drug-likeness and medicinal chemistry friendliness of small molecules. *Scientific Reports*, **2017**, 7(1), 42717.
[15] Maharana, D.K.C., Acharya, S.C. International Journal of Research Publication and Reviews. *International Journal of Research Publication and Reviews,* **2023**,
[16] Dhaliwal, J.S., Moshawih, S., Goh, K.W., Loy, M.J., Hossain, M.S., Hermansyah, A., Dhaliwal, S.K.S. Pharmacotherapeutics applications and chemistry of chalcone derivatives. *Molecules*, **2022**, 27(20), 7062.
[17] Szydło, Z.A. The beginnings of chemistry: from ancient times until 1661. *Pure and Applied Chemistry*, **2022**, 94(7), 869-888.
[18] Suharoschi R, Pop OL, Ciont C, Muresan CI, Heghes SC. Chalcones. In: Jafari SM, Rashidinejad A, Simal-Gandara J, editors. Handbook of Food Bioactive Ingredients: Properties and Applications. *Springer Cham*, **2023**, 365–406.
[19] Donaire-Arias, A., Poulsen, M.L., Ramón-Costa, J., Montagut, A.M., Estrada-Tejedor, R., Borrell, J.I. Synthesis of Chalcones: An Improved High-Yield and Substituent-Independent Protocol for an Old Structure. *Molecules*, **2023**, 28(22), 7576.
[20] Mondal D.S., Dr Sumanta , Dr. Sumanta Mondal _ Lecture Notes _Pharmaceutical Organic Chemistry-I Practical (BP 208P)_B.Pharm-II Sem. **2022**.
[21] Pagadala, R., Kasi, V., Shabalala, N.G., Jonnalagadda, S.B. Ultrasound-assisted multicomponent synthesis of heterocycles in water–A review. *Arabian Journal of Chemistry*, **2022**, 15(1), 103544.
[22] Tiwari, A., Bendi, A., Bhathiwal, A.S. An overview on synthesis and biological activity of chalcone derived pyrazolines. *Chemistry Select*, **2021**, 6(45), 12757-12795.
[23] Wan, L., Kong, G., Liu, M., Jiang, M., Cheng, D., Chen, F. Flow chemistry in the multi-step synthesis of natural products. *Green Synthesis and Catalysis*, **2022**, 3(3), 243-258.
[24] Farooq, S., Ngaini, Z. One pot and two pot synthetic strategies and biological applications of epoxy-chalcones. *Chemistry Africa*, **2020**, 3(2), 291-302.
[25] de la Hoz, A., Alkorta, I., Elguero, J. The mechanism of the reaction of hydrazines with α, β-unsaturated carbonyl compounds to afford hydrazones and 2-pyrazolines (4, 5-dihydro-1H-pyrazoles): Experimental and theoretical results. *Tetrahedron*, **2021**, 97, 132413.
[26] Costa, P., Pilli, R., Pinheiro, S., Bakuzis, P. Chemistry of Carbonyl Compounds and Derivatives. ed. *Royal Society of Chemistry*, **2022**.
[27] Pedretty K, Tillett K, Tsuei W, Lopchuk JM. Five-membered ring systems: pyrroles and benzo analogs. In: *Progress in Heterocyclic Chemistry Elsevier*, **2021**, 193–240.
[28] Matiadis, D., Nowak, K.E., Alexandratou, E., Hatzidimitriou, A., Sagnou, M., Papadakis, R. Synthesis and (fluoro) solvatochromism of two 3-styryl-2-pyrazoline derivatives bearing benzoic acid moiety: A spectral, crystallographic and computational study. *Journal of Molecular Liquids*, **2021**, 331,115737.
[29] Ramesh, D., Joji, A., Vijayakumar, B.G., Sethumadhavan, A., Mani, M., Kannan, T. Indole chalcones: Design, synthesis, in vitro and in silico evaluation against Mycobacterium tuberculosis. *European Journal of Medicinal Chemistry*, **2020**, 198, 112358.
[30] Bakchi, B., Krishna, A.D., Sreecharan, E., Ganesh, V.B.J., Niharika, M., Maharshi, S., Shaik, A.B. An overview on applications of SwissADME web tool in the design and development of anticancer, antitubercular and antimicrobial agents: a medicinal chemist's perspective. *Journal of Molecular Structure*, **2022**, 1259, 132712.
[31] Kondapuram, S.K., Sarvagalla, S., Coumar, M.S. Docking-based virtual screening using

PyRx Tool: autophagy target Vps34 as a case study. In *Molecular Docking for Computer-Aided Drug Design*, **2021**, 463-477.
[32] Ayodele, P.F., Bamigbade, A., Bamigbade, O.O., Adeniyi, I.A., Tachin, E.S., Seweje, A.J., Farohunbi, S.T. Illustrated procedure to perform molecular docking using PyRx and Biovia discovery studio visualizer: a case study of 10kt with atropine. *Progress in Drug Discovery & Biomedical Science*, **2023**, 6(1).
[33] Zainuddin, A., Hidayat, I.W., Kurnia, D., Ramadhanty, Z.F., Padilah, R. Prediction of the mechanism of action of catechin as superoxide anion antioxidants and natural antivirals for COVID-19 infection with in silico study. *Journal of Advanced Pharmaceutical Technology & Research*, **2022**, 13(3), 191-196.
[34] HDT, M. In vitro anti-inflammatory egg albumin denaturation assay: An enhanced approach. *Journal of Natural & Ayurvedic Medicine*, **2023**, 7(3), 1-6.
[35] Chaiya, P., Senarat, S., Phaechamud, T., Narakornwit, W. In vitro anti-inflammatory activity using thermally inhibiting protein denaturation of egg albumin and antimicrobial activities of some organic solvents. *Materials Today: Proceedings*, **2022**, 65, 2290-2295.
[36] Baliyan S, Mukherjee R, Priyadarshini A, Vibhuti A, Gupta A, Pandey RP, Chang CM. Determination of Antioxidants by DPPH Radical Scavenging Activity and Quantitative Phytochemical Analysis of *Ficus religiosa*. *Molecules*, **2022**, 27(4), 1326.
[37] Siddiqui, F., Makhloufi, R., Salah, M.E.-S., Mohamed, E., Hojjati, M. Computational Exploration of Quinine and Mefloquine as Potential Anti-Malarial Agents. *Journal of Pharmaceutical Sciences and Computational Chemistry*, **2025**, 1(2), 106-115.
[38] Tamboli, A., Tayade, S. In-Depth Investigation of Berberine and Tropane through Computational Screening as Possible DPP-IV Inhibitors for the Treatment of T2DM. *Journal of Pharmaceutical Sciences and Computational Chemistry*, **2025**, 1(1), 1-11.
[39] Madhuranga, H., Samarakoon, D. Advancing in vitro antioxidant activity assessment: a comprehensive methodological review and improved approaches for DPPH, FRAP and H2O2 assays. *Nat Ayurvedic Med*, **2023**, 7(4), 000431.

Graphical Abstract



Copyright © 2025 by authors and SPC (Sami Publishing Company) + is an open access article distributed under the Creative Commons Attribution License(CC BY), which permits unrestricted use, distribution, and reproduction in any medium, provided the original work is properly cited.